PERGAMON

Journal of Atmospheric and Solar-Terrestrial Physics 63 (2001) 513–522

Journal of ATMOSPHERIC AND SOLAR-TERRESTRIAL PHYSICS

www.elsevier.nl/locate/jastp

Auroral zone dayside precipitation during magnetic storm initial phases

B.T. Tsurutani[a,*], X.-Y. Zhou[a], J.K. Arballo[a], W.D. Gonzalez[b], G.S. Lakhina[c], V. Vasyliunas[d], J.S. Pickett[e], T. Araki[f], H. Yang[g], G. Rostoker[h], T.J. Hughes[h], R.P. Lepping[i], D. Berdichevsky[i]

[a] *Jet Propulsion Laboratory, California Institute of Technology, 4800 Oak Grove Drive, Pasadena, CA 91109-8099, USA*
[b] *INPE-Caixa Postal 515, 12200 Sao Jose Dos Campos, Sao Paulo, Brazil*
[c] *Indian Institute of Geomagnetism, Colaba, Mumbai 400 005, India*
[d] *Max-Planck-Institut für Aeronomie, 3411 Katlenburg, D 3411, Lindau, Germany*
[e] *Department of Physics & Astronomy, University of Iowa, Iowa City, IA, USA*
[f] *Department of Geophysics, Kyoto University, Kyoto 606, Japan*
[g] *National Institute of Polar Research, 1-9-10 Kaga, Itabashi-ku, Tokyo 173, Japan*
[h] *Technical Communication and Services, Ottawa, Ont. K2A 2V1, Canada*
[i] *Goddard Space Flight Center, Code 696, Greenbelt, MD, USA*

Received 11 October 1999; received in revised form 31 March 2000; accepted 7 April 2000

Abstract

Significant charged-particle precipitation occurs in the dayside auroral zone during and after interplanetary shock impingements on the Earth's magnetosphere. The precipitation intensities and spatial and temporal evolution are discussed. Although the post-shock energy flux (10–20 erg cm^{-2} s^{-1}) is lower than that of substorms, the total energy deposition rate may be considerably greater ($\sim$ an order of magnitude) than nightside energy rates due to the greater area of the dayside portion of the auroral oval (defined as extending from 03 MLT through noon to 21 MLT). This dayside precipitation represents direct solar wind energy input into the magnetosphere/ionosphere system. The exact mechanisms for particle energization and precipitation into the ionosphere are not known at this time. Different mechanisms are probably occurring during different portions of the storm initial phase. Immediately after shock compression of the magnetosphere, possible precipitation-related mechanisms are: (1) betatron compression of preexisting outer zone magnetospheric particles. The anisotropic plasma is unstable to loss-cone instabilities, leading to plasma wave growth, resonant particle pitch-angle scattering and electron and proton losses into the upper ionosphere. (2) The compression of the magnetosphere can also lead to enhanced field-aligned currents and the formation of dayside double-layers. Finally (3) in the latter stages of the storm initial phase, there is evidence for a long-lasting viscous-like interaction occurring on the flanks of the magnetopause. Ground-based observations identifying the types of dayside auroral forms would be extremely useful in identifying the specific solar wind energy transfer mechanisms.

Keywords: Aurora; Magnetic storms; Magnetosphere

1. Introduction

The primary physical process of solar wind energy transfer to the magnetosphere for the main phase of major magnetic storms is believed to be magnetic reconnection (Gonzalez and Tsurutani, 1987; Gonzalez et al., 1989,1994; Kamide et al., 1998). This process involves field-line merging at the magnetopause, transport of magnetic flux and plasma to the magnetotail, further reconnection in the tail neutral sheet, and transport back to the nightside magnetosphere (Dungey, 1961). The southwardly directed

* Corresponding author.
E-mail address: btsurutani@jplsp.jpl.nasa.gov (B.T. Tsurutani).

1364-6826/01/$ - see front matter
PII: S1364-6826(00)00161-9

and long-duration intense magnetic fields in both the sheath ahead of a fast interplanetary coronal mass ejection (ICMEs) and in magnetic clouds within ICMEs (Burlaga et al., 1981; Lepping et al., 1990), lead to intense storm main phases (Tsurutani and Gonzalez, 1997; Tsurutani et al., 1999).

Unfortunately, storm "initial phases" have been neglected in magnetic storm studies (there are no articles dealing with this topic in the "Magnetic Storm" monograph or the *J. Geophys. Res.*, 1997 special issue on magnetic storms). Joselyn and Tsurutani (1990) have argued that the term "storm sudden commencement" (SSC) is a misnomer and should simply be called a sudden impulse (SI). Their reasoning was that SIs are simply created by interplanetary shock compressions of the magnetosphere (Smith et al., 1986), and there is no physical difference between shocks that create SIs and those that are followed by large southward fields (leading to storm main phases). Earlier, Rostoker and Falthammar (1967) had suggested that storm initial and main phases be treated as separate disturbances. In accordance, Sugiura (private communication, 1999) suggested that the "storm initial phase" is not actually a part of the magnetic storm itself, and should be renamed.

The purpose of this paper is to demonstrate that there is significant solar wind energy transfer to the magnetosphere–ionosphere system during and after interplanetary shock impingement at the Earth's magnetosphere and that the importance of storm initial phases should be reconsidered. The amount of energy precipitation is substantial, and cannot be ignored. Significant dayside auroral energy deposition is caused by interplanetary shocks (Zhou and Tsurutani, 1999). The interplanetary shock-associated dayside auroras involve not only the dayside auroral brightenings but an expansion of this aurora from noon to 03 and 21 MLT, associated with the shock downtail propagation. The same energization and precipitation effects are expected to occur for SI events (shocks not followed by IMF B_S events). However, if enhanced ionospheric conductivity affects subsequent geomagnetic activity (as suggested by Kan et al., 1988), then the precipitation occurring in storm initial phases may indeed affect the subsequent storm main phases. Gonzalez et al. (1990) have shown that there is an intensity difference between storms caused by B_S–B_N magnetic clouds and those caused by B_N–B_S clouds, with the latter cases being less intense. This may simply be due to a storm initial phase ionospheric priming effect, discussed above. A second related possible explanation is a plasma sheet priming effect (Borovsky et al., 1998).

2. Data analysis procedure

We use the WIND magnetic field and plasma parameters to characterize the upstream solar wind. The magnetometer experiment is described in Lepping et al. (1995) and the plasma detector in Ogilvie et al. (1995). The auroral zone energy is derived from POLAR UV imaging data. The UV imaging experiment is described in Torr et al. (1995). The LBH-long passband centered at 170 nm is used in this study. This band emission, with a corresponding peak emission altitude of ~120 km, is relatively insensitive to the characteristic energy of the precipitating electrons and is dependent primarily on the total energy flux (Lummerzheim et al., 1997). The conversion from photon flux to surface brightness (in Rayleighs) for each pixel is a factor of $4\pi/(\Omega 10^6) \approx 30.17$, where Ω is the solid angle subtended by a single pixel (4.17×10^{-7} sr) (Brittnacher et al., 1997). A relationship between the surface brightness and auroral electron energy flux can be determined by one-dimensional transport models that calculate column-integrated intensities from incident auroral electrons. Germany et al. (1994) and Lummerzheim et al. (1997) estimate this to be 110 Rayleighs per erg cm^{-2} s^{-1}.

The arrival time of the interplanetary shocks at the magnetopause can be determined by two different methods. The shock velocity in the plasma frame can be calculated using the Rankine–Hugoniot conservation equations (as shown in Tsurutani and Lin, 1985). With knowledge of the spacecraft position relative to the Earth and the shock normal angle, the delay time can be estimated. The accuracy of such estimations is often better than 1 min (Ho et al., 1998). Secondly, it has been noted that dayside auroral brightenings occur just after shock compression of the frontside magnetosphere (Craven et al., 1986; Tsurutani et al., 1998a; Arballo et al., 1998; Spann et al., 1998; Zhou and Tsurutani, 1999). The POLAR UV cadences used in this study is an image every ~3 min (for the January 10, 1997 event) and an image every ~37 s (for the September 24, 1998 event), so the shock arrival time uncertainty from this method is ±3 min and ±37 s, respectively. The image integration time is 37 s. In this paper, we use both methods to identify the arrival times of the shocks at the magnetopause.

3. Results

3.1. January 10, 1997 event

Abrupt increases in the solar wind density, temperature, and velocity and an increase in field strength are characteristics of jump conditions across fast-forward shocks (Kennel et al., 1985). Kennel et al. (1985) have shown theoretically that the density and magnetic field compression are closely related to the shock magnetosonic Mach number ($V_{shock}/V_{magnetosonic}$). The density and field compression values are approximately equal to the Mach number, up to a value of Mach 4. In interplanetary space at 1 AU, Tsurutani and Lin (1985) showed that the typical Mach number for shocks ahead of fast ICMEs is typically 1.5–3. Only rarely does one detect an interplanetary Mach 4.0 shock or higher. Thus, although both the density and speed increase across an interplanetary shock, it is the density increase that

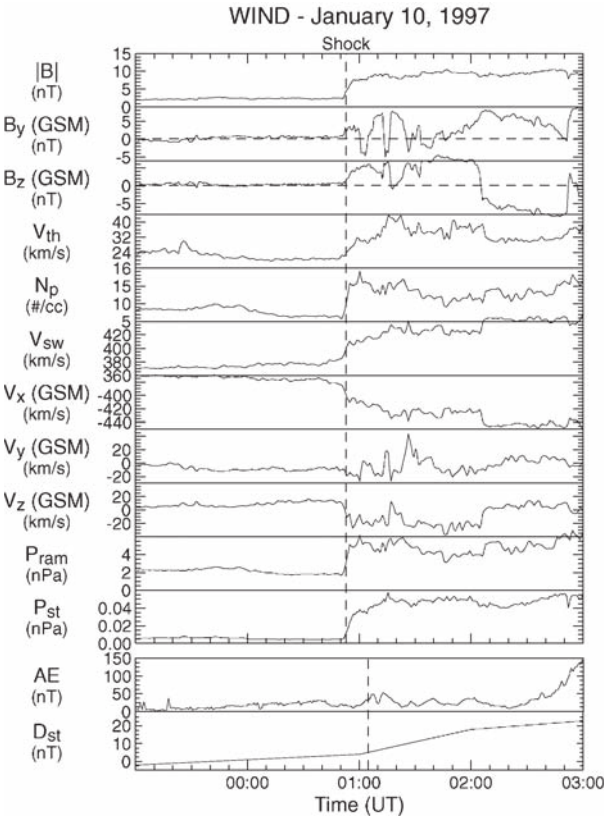

Fig. 1. The January 10, 1997 interplanetary shock events. An interplanetary shock is observed by WIND at 0052 UT (the dashed line). At the time, WIND was located at $(85, -59, -3)\,R_e$ upstream of the Earth in GSE coordinates.

typically plays the key role in the ram pressure ($N_i m_i V_{sw}^2$) increase.

Fig. 1 shows the fast-forward shock (dashed vertical line) on January 10, 1997 observed by WIND at 0052 UT at an upstream distance of $\sim 85 R_e$. This event and the resultant geomagnetic activity was studied in great detail by the ISTP community (ISTP Sun–Earth Connections; Spann et al., 1998). The shock had a Mach number of ~ 1.5 (Berdichevsky et al., 2000). In Fig. 1, both $|\mathbf{B}|$ and N_p have increases ~ 2 times the upstream values. At the interplanetary shock, the IMF B_y changes from ~ 1.0 to ~ 3.5 nT, and the B_z component increases from zero to ~ 4 nT. The solar wind bulk speed jumps from ~ 380 to ~ 410 km s^{-1} across the shock. The ram pressure increases from ~ 2 to ~ 5 nPa across the shock, a factor of ~ 2.5 increase.

The bottom two panels of Fig. 1 are the geomagnetic indices AE and D_{ST}. The vertical dashed line is time shifted to show when the interplanetary shock arrives at the magnetopause. The minor AE disturbances are associated with pseudobreakups in the nightside (Arballo et al., 1998 and Zhou and Tsurutani, 2000). The increase in D_{ST} shows the initial phase of this storm (D_{ST} is an hourly index). This initial phase lasts several hours until 0500 UT, January 10, 1997 (not shown).

Fig. 2 shows the interplanetary shock effects on the auroral ionosphere. The POLAR UV images evolve in time from left-to-right and top-to-bottom. The beginning of each of the ~ 37 s cadence images is indicated at the top of each frame. The geomagnetic north pole is at the center of each image with 60° magnetic latitude noon at the top. Local dawn is to the right and dusk on the left. In the top left-most two images (before the IP shock arrival), there is some precipitation between ~ 3 and ~ 15 MLT. There is far less precipitation near local midnight. The IMF B_y and B_z components were close to zero at this time. The interplanetary shock arrives just prior to the time of image (c). On image (c), a substantial brightening of the aurora is noted (at ~ 0107 UT). Shown in panels (c)–(h) of Fig. 2, the shock-related aurora expands in the antisunward direction toward the dawn and dusk and even approaches the midnight sector. By the shock arrival time at the magnetopause plus 13 min, the aurora has evolved into an asymmetric "horseshoe" shape. The "dayside" aurora extends from ~ 0230 through noon to ~ 2200 MLT. The aurora is brighter on the dawnside (note the enhancement at ~ 0700 LT at 75° latitude) than on the duskside. There is relatively little precipitation near midnight.

The shock normal θ_{nx} angle (the angle between the shock normal and the negative x-axis) and the shock velocity have been determined to be 20 ± 3° and 503 ± 10 km s^{-1}, respectively (Berdichevsky et al., 1999). Thus the delay time of the shock is calculated to be $\tau = X/V_{shock} \cos\theta_{nx} \approx 15$ min. So the calculated shock arrival time is ~ 0107 UT, which is consistent with the UVI observations shown in Fig. 2(c).

Fig. 3 shows the northern hemisphere aurora at times well beyond those of Fig. 2 (but still in the storm initial phase). From 0223 UT (top left panel) until 0325 UT (bottom row, second image from the left), an inverted "horseshoe-shaped" aurora develops during a southward IMF B_z event lasting from ~ 0205 to 0251 UT at WIND (as shown by Fig. 1). (There is also significant polar cap aurora present, but we will not discuss this topic here.) This occurs in the storm initial phase and has been discussed in detail in Tsurutani et al. (1998a). By 0300 UT, the aurora is nearly uniform, other than the absence of aurora near local noon. There are no particularly noteworthy auroral features at local midnight from 0223 to 0327 UT. At ~ 0334 UT, a substorm expansive phase onset occurs (small brightening at local midnight). By 0337 UT, the substorm is readily apparent (see Tsurutani et al., 1998b).

From Fig. 1, at ~ 0253 UT the IMF B_z turns abruptly northward. The field rotates southward and then turns northward once again at 0306 UT to ~ 8 nT and this lasts ~ 15 min. Using the observed solar wind speed, a convection time of ~ 14 min from the WIND spacecraft to the dayside magnetopause is calculated. Thus, this second IMF B_z northward turning arrival time is at ~ 0320 UT. The delay time between the arrival time and the substorm onset is ~ 14 min. This timing is close to but outside the statistical range of B_N triggering discussed by Lyons et al. (1997).

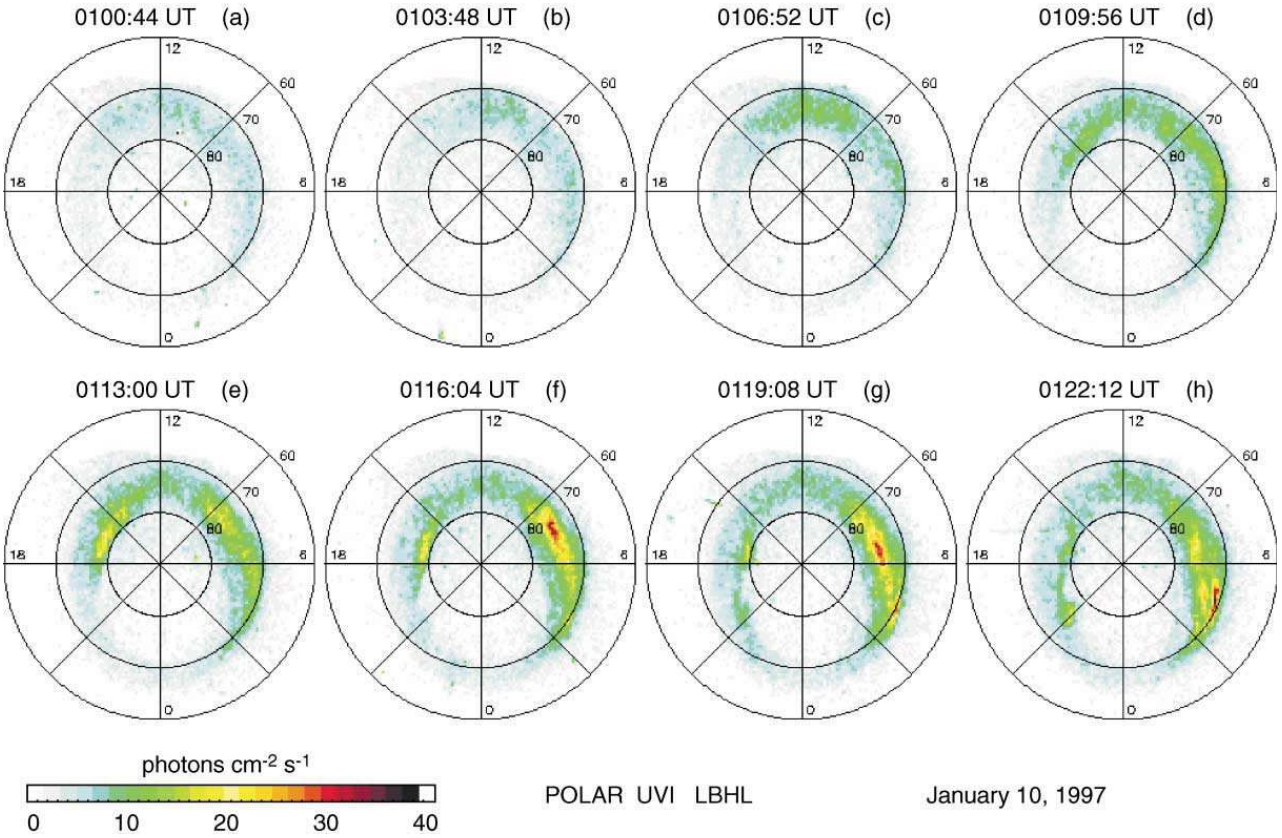

Fig. 2. POLAR UV images of the dayside aurora prior to and after shock compression of the magnetosphere. The time sequence goes from left to right and down. A magnetic coordinate system is used with magnetic local noon at the top and dawn at the right of the images. The linear color scale indicates the photon flux (photons cm^{-2} s^{-1}) collected in the instrumentation aperture due to optical emission within a single pixel at the emission region.

3.2. September 24, 1998 event-energy calculation

The September 24, 1998 interplanetary shock event is shown in Fig. 4. At the shock, the magnetic field increases from ~13 to ~40 nT, the IMF B_z changes from −2 to 6 nT, and the density increases from ~8 to ~20 cm^{-3}. As shown in the bottom two panels, the ram pressure increases from ~4 to ~16 nPa, and the static pressure increases from 0.1 to 0.9 nPa. The issue of substorm triggering by effects of these pressure increases is discussed elsewhere by Zhou and Tsurutani (2000). For this shock event, Russell et al. (2000) have determined that the shock normal direction is $(-0.973, -0.217, -0.059)$ in GSE coordinates. The shock speed is 756 km s^{-1} and the Mach number is ~2.9. They have predicted that this interplanetary shock will reach the magnetopause $(10, 0, 0)R_e$ at 2344:19 UT with an estimated error of ±20 s. The geosynchronous spacecraft GOES 10 (located at 15 LT) detected interplanetary shock compression effects at 2344:10 UT.

Although somewhat beyond the main scope of this paper, the interplanetary shock also triggers substorm intensifications (Zhou and Tsurutani, 2000). The geomagnetic response is shown in the bottom panels of Fig. 4. The (shifted) dashed line is the time when the interplanetary shock arrives at the magnetopause. Abrupt AE index intensification occurs at 2346:30 UT from ~700 to ~1200 nT and reaches to ~2000 nT at 2348:30 UT. The substorm is delayed by ~2.5 min.

The POLAR UV images associated with the interplanetary event are given in Fig. 5. The left two images (panels a and b) were taken prior to the shock arrival, the third one (panel c) just after shock arrival, and the one on the far right, ~2 min after the shock arrival. At 2344:07 UT (panel b) prior to shock arrival, there is clearly substorm energy deposition in a region centered near ~2100 MLT. It is present between ~62 and 69° latitude (i.e., within the auroral oval). At ~2344:44 UT, the dayside aurora brightens between 0900 and 1500 MLT. This auroral intensification indicates that the interplanetary shock arrived at the dayside magnetopause between ~2344:07 and ~2344:44 UT (for this event a ~37 s image cadence was available). The calculated arrival time of ~2344:19 UT is in excellent agreement with the imaging data. The dayside auroral intensification extends from 0300 to 1600 LT. Also note that there is an intensification of the nightside (substorm) aurora at ~2346:34 UT, which is in excellent agreement with the

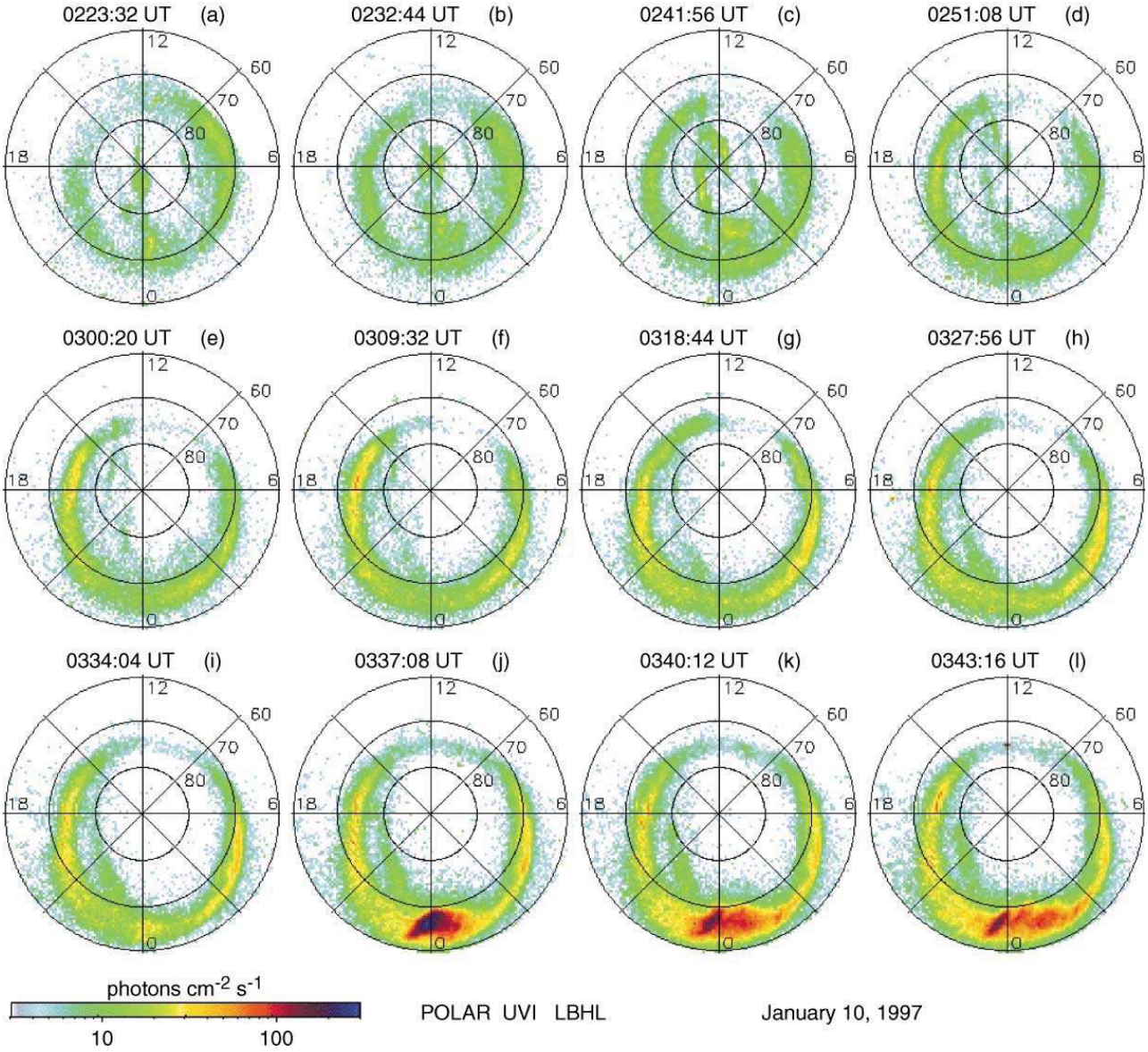

Fig. 3. The dayside horseshoe aurora $\sim 1-\frac{1}{2}$ h into the January 10, 1997 storm initial phase. Images are shown in geomagnetic coordinates. The time sequence goes from panel (a)–(l). The color bar shows the irradiance in logarithmic units.

AE enhancement as shown in Fig. 4. The substorm auroral brightening extends from 0200 MLT through midnight to 2000 MLT. Thus, the "substorm intensification" is complex and is not simply brightening of the preexisting substorm area (this subject is beyond the scope of the present paper, and will be addressed elsewhere).

Fig. 6 shows the "dayside" aurora at 2345:57 UT. In the image, both the dayside aurora and substorm aurora are encircled for calculation purposes (we are currently in the process of writing a program to identify auroral boundaries and to calculate the total auroral energy deposition rates. This is not yet completed). Relatively accurate estimates of energy deposition can be made by hand-analyses. We estimate that the uncertainty is ±30%. We calculate the energy deposition rates by estimating average deposition rates for a specific area and then measure the area. We find that the average energy flux intensity for the dayside aurora is ~10–20 erg cm^{-2} s^{-1} and for substorms, ~30–40 erg cm^{-2} s^{-1}. The total dayside area is $\sim 7.5 \times 10^{16}$ cm^2 while that of the demarcated substorm region is $\sim 9.2 \times 10^{15}$ cm^2. Thus the total energy deposition rates are $0.8–1.5 \times 10^{18}$ erg s^{-1} and $2.8–3.7 \times 10^{17}$ erg s^{-1} for the dayside aurora and substorm aurora, respectively. The dayside energy deposition rate is ~3–4 times greater than that of the substorm.

In the above, we did not take into account the errors resulting from non-vertical viewing. From the satellite position of $7.9R_e$ to the ionosphere, the angles of viewing for

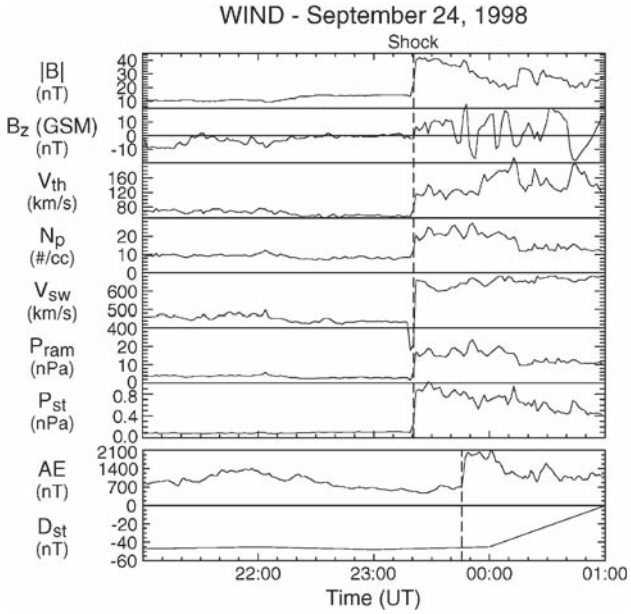

Fig. 4. The interplanetary shock of September 24, 1998. The IP shock is observed by WIND at 2320 UT at $(183, 15, -6)R_e$ upstream of the Earth in GSE coordinates.

the noon and midnight sectors are $\sim 73^\circ$ and $\sim 80^\circ$ latitude, respectively. This small difference will result in an insignificant difference relative to the "3–4 times" energy deposition rate quoted above.

4. Energization/ precipitation models

We attempt to outline several solar wind energy transfer mechanisms that may be responsible for the dayside aurora. It is possible that several different mechanisms might be taking place at the same time.

4.1. Adiabatic compression

A schematic representation of an adiabatic compression model (taken from Zhou and Tsurutani, 1999) is given in Fig. 7. The ram pressure increase across the shock compresses the frontside magnetosphere. Preexisting plasma on outer zone magnetospheric field lines becomes betatron accelerated/energized from the absorption of solar wind ram energy. By conservation of the first adiabatic invariant, $E_\perp/|\mathbf{B}|$, where $E_\perp$ is the particle perpendicular kinetic energy, magnetospheric compression lead to an increase in $E_\perp$. Because $E_{||}$ remains nearly constant, $E_\perp/E_{||} > 1$. This latter effect leads to loss-cone instabilities with the growth of plasma waves and concomitant electron and proton pitch angle scattering. The particles that get scattered into the loss cone have collisions with upper ionosphere atoms and molecules and lose most of their energy by electron excitation. The subsequent atomic and molecular decays lead to the auroras.

Olsen and Lee (1983) and Anderson and Hamilton (1993) have noted enhanced electromagnetic ion–cyclotron waves and Lauben et al. (1998) enhanced electromagnetic whistler mode chorus emissions during magnetospheric compression events. These results support the above scenario for the onset of dayside proton and electron loss-cone instabilities during shock compression events, respectively. However, a direct relationship between shock compression, plasma waves and aurora has not been made to date. We plan on making such tests in the near future.

4.2. Field-aligned current intensifications

Shock compression of the magnetosphere may also lead to intensification of field-aligned currents (Araki, 1994; Lysak et al., 1995). A schematic representation is shown in Fig. 8. If current-driven instabilities (Lakhina and

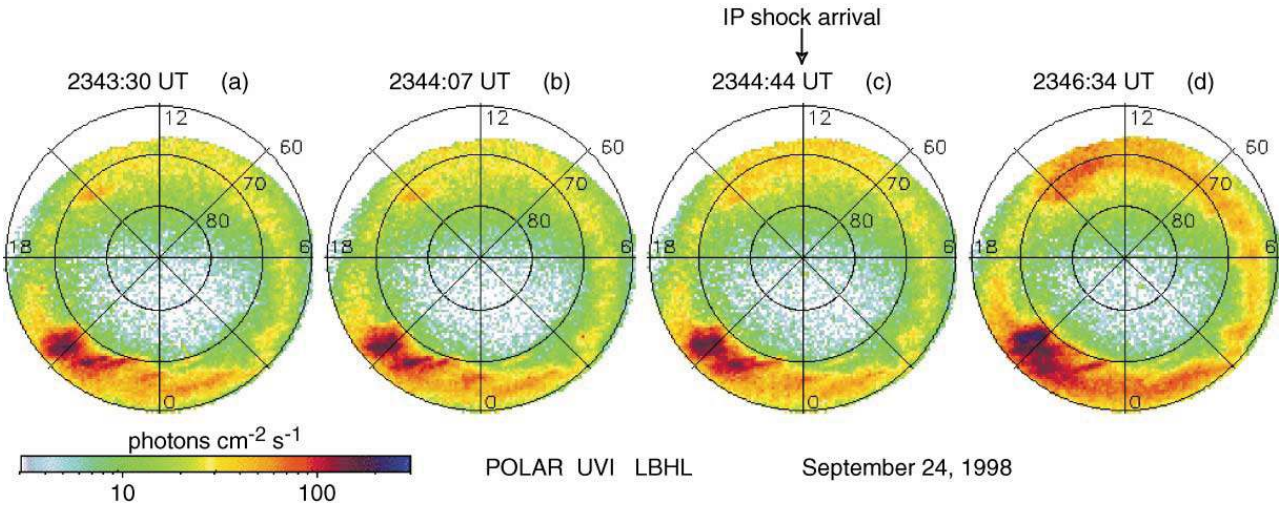

Fig. 5. Same as Fig. 2, but for the September 24, 1998 shock event.

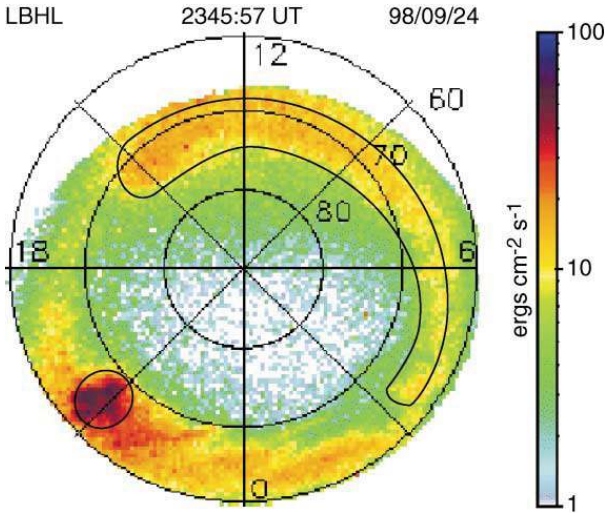

Fig. 6. The dayside aurora and a nightside substorm. The total dayside energy disposition rate is ~3–4 times that of the substorm.

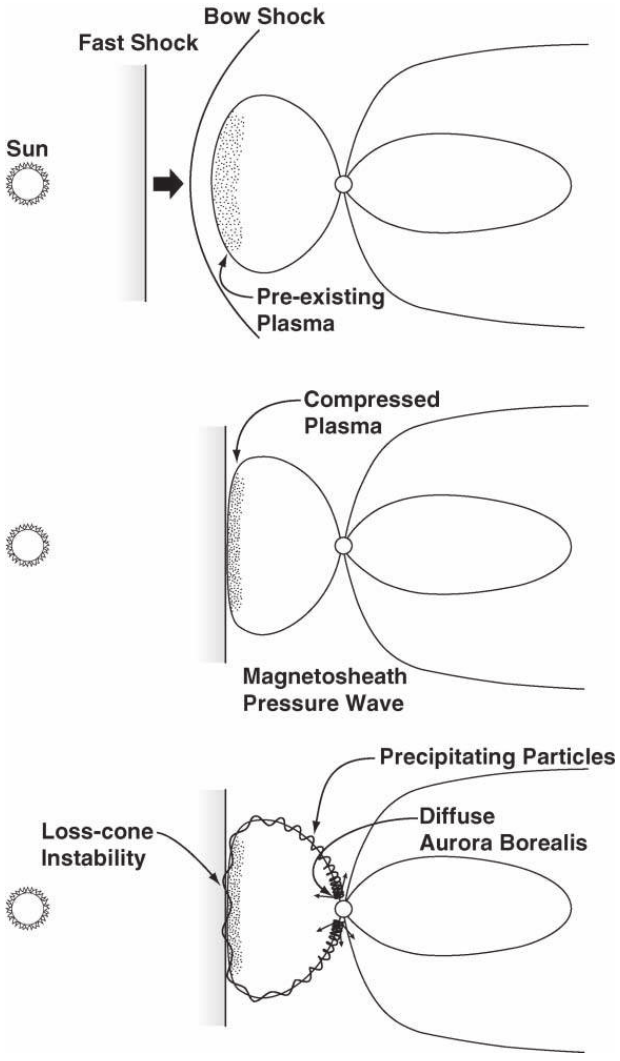

Fig. 7. A schematic representation of adiabatic compression of dayside magnetospheric plasma.

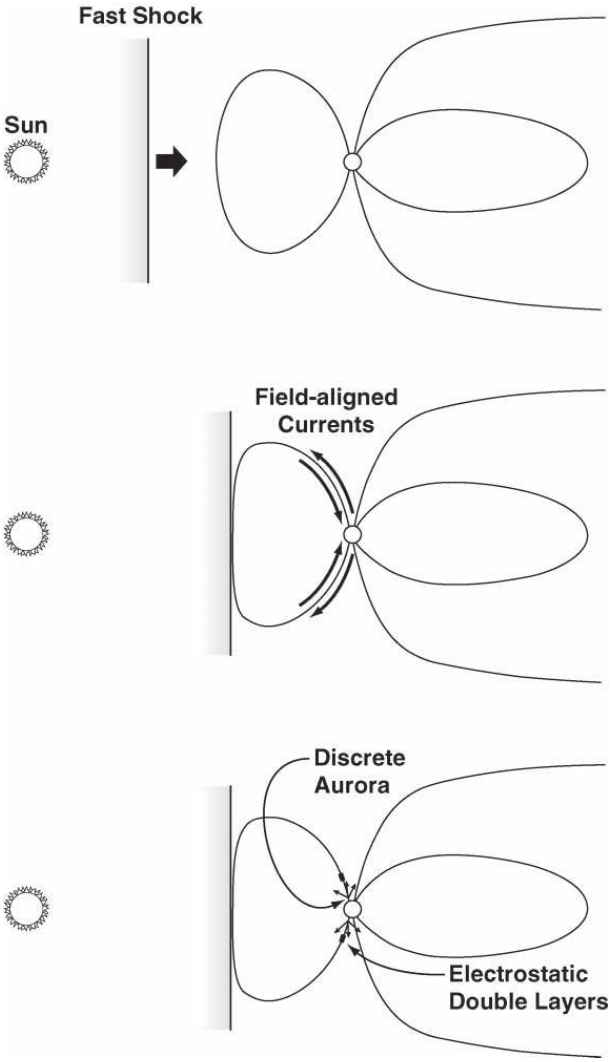

Fig. 8. A schematic representation of dayside field-line current intensification.

Tsurutani, 1999) are caused by this mechanism, depending upon the ion to electron temperature ratio, T_i/T_e, either electrostatic ion acoustic waves or lower hybrid waves are expected to have strong growth rates. The turbulence due to current-driven instabilities could enhance anomalous resistivity, which could then support large parallel electric fields along auroral zone field lines. These parallel electric fields can accelerate charged particles, and downward accelerated electrons can produce intense aurora. Alternatively, the nonlinear development of these waves may lead to the generation of double-layers and the acceleration of auroral particles close to the ionosphere.

Do double-layers occur on the dayside? A statistical study of auroral solitary waves and weak double layers (Mälkki et al., 1993) indicates that both types of phenomena are present on the dayside (see their Figs. 3 and 4). However, at this time, a direct association between interplanetary shocks and dayside double-layers has not been investigated.

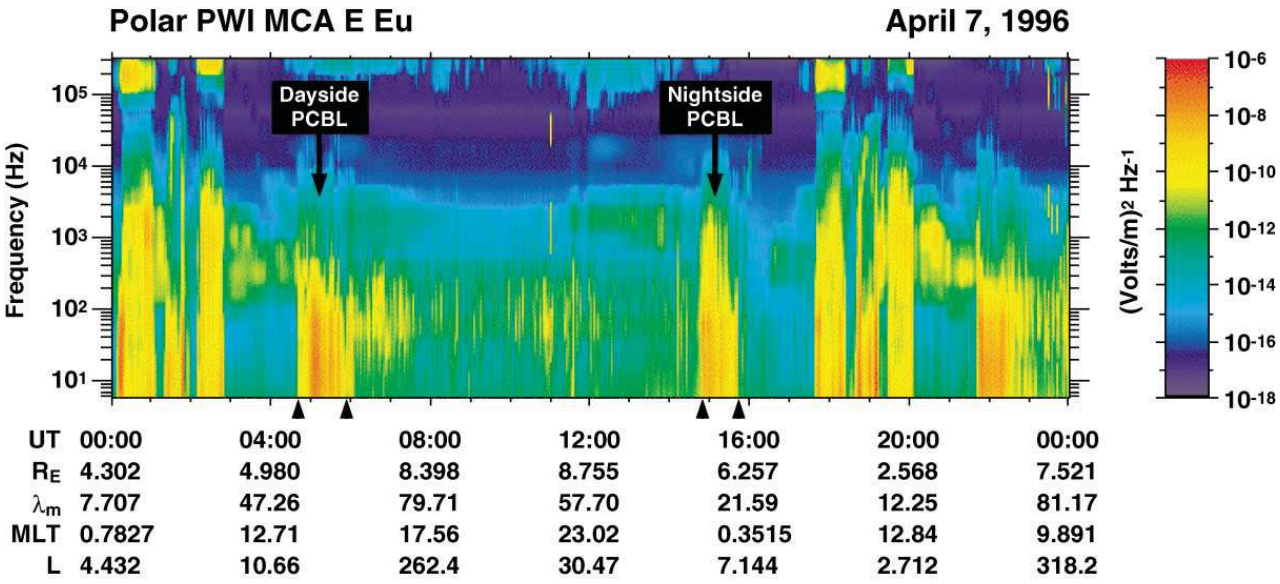

Fig. 9. ELF/VLF PCBL boundary layer waves detected by POLAR. The dayside and nightside waves are indicated by arrows. These "broadband" emissions may be related to viscous interaction at the magnetopause, with the result of the dayside aurora of the type shown in Fig. 3.

How can one distinguish between these two models? It is clear that both plasma compression and field-aligned current intensification occur associated with shock compression events. Clearly, field and plasma compressions take place, but whether or not the loss-cone instabilities are sufficiently strong to lead to significant particle losses to explain the dayside aurora is not known at this time. "Diffuse" aurora would be associated with this specific process.

Intensification of field-aligned currents associated with interplanetary shock compression has been previously proposed in a model of geomagnetic sudden commencements (Araki, 1994). Whether or not this leads first to field-aligned current instabilities (Lakhina and Tsurutani, 1999) and then to the formation of double-layers on the dayside is not known. The aurora associated with this mechanism would be expected to be arc-like displays. However, Lysak and Lee (1992) and Lysak et al. (1995) have pointed out that the generation and propagation of field-aligned currents by solar wind dynamic pressure pulses is a major magnetopause–ionosphere coupling mechanism. These authors suggested that the currents propagate as shear mode Alfvén waves and that they can have associated parallel potential drops, which then can accelerate the electrons required to produce the observed optical signatures.

4.3. Viscous interaction

It was noted that the dayside aurora can be present many hours after shock passage, well into the initial phase of a magnetic storm. This occurred when the IMF B_z was negative. The local time signature of the aurora was that expected from a viscous-like solar-wind–magnetosphere interaction. There were weak or no auroras near noon, and a bright aurora at dawn, dusk and midnight. The aurora was continuous and had a horseshoe shape. It is doubtful that either of the two shock-related mechanisms discussed previously could

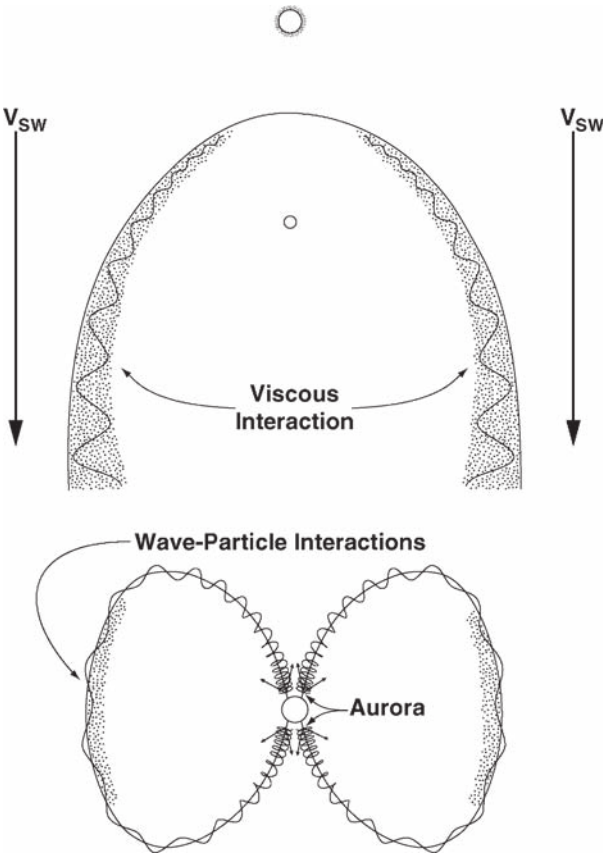

Fig. 10. A schematic representation of viscous interaction.

account for these displays. The bounce times of energetic ~1–10 keV electrons and ions are seconds and minutes, respectively, so compressed, preexisting particles should be lost after ~10 s or minutes. For field-aligned current enhancements, this would be expected just at the time of shock passage and the effects would be maximum at noon rather than at dawn or dusk. Thus, this latter mechanism seems unlikely to explain auroras near dawn and dusk hours after shock passage.

A more likely scenario is the development of a Kelvin–Helmholtz instability (Rostoker et al., 1992). This instability growth rate maximizes when the field lines of the magnetosheath and the magnetotail are orthogonal to the solar wind fields, as was the case here. Another possible mechanism is cross-field diffusion of magnetosheath plasma by ELF/VLF boundary layer waves. An example of waves detected by the POLAR spacecraft is shown in Fig. 9. The properties of these boundary layer waves are reviewed in Lakhina et al. (2000) and the cross-field diffusion process is discussed in Tsurutani and Lakhina (1997). A schematic representation of this mechanism is given in Fig. 10.

5. Conclusions

We have shown that there is significant energetic particle precipitation that occurs within the dayside auroral zone in the initial phases of magnetic storms. The mechanisms for particle energization and precipitation are currently unknown, but several likely possibilities are suggested. High temporal and spatial resolution ground-based imaging data will be extremely useful in resolving the issues of which mechanisms are in operation and which are most effective.

Acknowledgements

Portions of this work were done at the Jet Propulsion Laboratory, California Institute of Technology, under contract with the National Aeronautics and Space Administration. The research of G. Rostoker was supported by the Natural Sciences and Engineering Research Council of Canada. X.-Y. Zhou would like to thank the National Research Council for the award of a Resident Associateship at the Jet Propulsion Laboratory.

References

Anderson, B.J., Hamilton, D.C., 1993. Electromagnetic ion–cyclotron waves stimulated by modest magnetospheric compressions. Journal of Geophysical Research 98, 11 369.

Araki, T., 1994. A physical model of geomagnetic sudden commencement. In: Engebretson, M., Takahashi, K.T., Scholer, M. (Eds.), Solar Wind Sources of Ultra-Low-Frequency Wave Pulsations. American Geophysical Union, Washington, DC.

Arballo, J.K., Ho, C.M., Tsurutani, B.T., Zhou, X.-Y., Kamide, Y., Shue, J.-H., Akasofu, S.-I., Lepping, R.P., Goodrich, C.C., Papadopoulos, K., Sharma, A.S., Lyon, J.G., 1998. Pseudobreakups during January 10, 1997. In: Kokubun, S., Kamide, Y. (Eds.), Substorms-4. Kluwer Academic Publishers, Dordrecht.

Berdichevsky, D., Szabo, A., Lepping, R.P., Vinas, A.G., 2000. Interplanetary fast shocks and associated drivers observed through the twenty-third solar minimum by WIND over its first 2.5 years. Journal of Geophysical Research, in press.

Borovsky, J.E., Thomsen, M.F., Elphic, R.C., 1998. The driving of the plasma sheet by the solar wind. Journal of Geophysical Research 103, 17 617.

Brittnacher, M., Elsen, R., Parks, G., Chen, L., Germany, G., Spann, J., 1997. A dayside auroral energy deposition case study using the Polar Ultraviolet Imager. Geophysical Research Letters 24, 991.

Burlaga, L.F., Sittler, E., Mariani, F., Schwenn, R., 1981. Magnetic loop behind an interplanetary shock: Voyager, Helios and IMP-8 observations. Journal of Geophysical Research 86, 6673.

Craven, J.D., Frank, L.A., Russell, C.T., Smith, E.J., Lepping, R.P., 1986. Global auroral responses to magnetospheric compressions by shocks in the solar wind: two case studies. In: Kamide, Y., Slavin, J.A. (Eds.), Solar Wind–Magnetosphere Coupling. Terra Scientific Publishing Company, Tokyo, Japan.

Dungey, J.W., 1961. Interplanetary magnetic field and the auroral zones. Physical Review Letters 6, 47.

Germany, G.A., Torr, M.R., Torr, D.G., Richards, P.G., 1994. Use of FUV auroral emissions as diagnostic indicators. Journal of Geophysical Research 99, 383.

Gonzalez, W.D., Tsurutani, B.T., 1987. Criteria of interplanetary parameters causing intense magnetic storms ($D_{ST} < -100$ nT). Planetary and Space Science 35, 1101.

Gonzalez, W.D., Tsurutani, B.T., Gonzalez, A.L.C., Smith, E.J., Tang, F., Akasofu, S.-I., 1989. Solar wind magnetosphere coupling during intense magnetic storms (1978–1979). Journal of Geophysical Research 94, 8835.

Gonzalez, W.D., Lee, L.C., Tsurutani, B.T., 1990. Comments on the polarity of magnetic clouds. Journal of Geophysical Research 95, 17 267.

Gonzalez, W.D., Joselyn, J.A., Kamide, Y., Kroehl, H.W., Rostoker, G., Tsurutani, B.T., Vasyliunas, V.M., 1994. What is a geomagnetic storm?. Journal of Geophysical Research 99, 5771.

Ho, C.M., Tsurutani, B.T., Zhou, X.-Y., Arballo, J.K., Lepping, R.P., 1998. Interplanetary causes of the January 10, 1997 substorm event. Physics of Space Plasmas, Cambridge, MA, 15, 157.

Joselyn, J.A., Tsurutani, B.T., 1990. Geomagnetic Sudden impulses and storm sudden commencements: a note on terminology. EOS 71, 1808.

Kamide, Y., Baumjohann, W., Daglis, I.A., Gonzalez, W.D., Grande, M., Joselyn, J.A., McPherron, R.L., Phillips, J.L., Reeves, E.G.D., Rostoker, G., Sharma, A.S., Singer, H.J., Tsurutani, B.T., Vasyliunas, V.M., 1998. Current understanding of magnetic storms: storm-substorm relationships. Journal of Geophysical Research 103, 17 705.

Kan, J.R., Zhu, L., Akasofu, S.-I., 1988. A theory of substorms: onset and subsidence. Journal of Geophysical Research 93, 5624.

Kennel, C.F., Edmiston, J.P., Hada, T., 1985. A quarter century of collisionless shock research. In: Stone, R.G., Tsurutani, B.T.

(Eds.), Collisionless Shocks in the Heliosphere: A Tutorial Review. American Geophysical Union, Washington, DC.

Lakhina, G.S., Tsurutani, B.T., 1999. A generation mechanism for the polar cap boundary layer broadband plasma waves. Journal of Geophysical Research 104, 279.

Lakhina, G.S., Tsurutani, B.T., Kojima, H., Matsumoto, H., 2000. "Broadband" plasma waves in the boundary layers. Journal of Geophysical Research, in press.

Lauben, D.S., Inan, U.S., Bell, T.F., Kirchner, D.L., Hospodarsky, G.B., Pickett, J.S., 1998. VLF chorus emissions observed by POLAR during the January 10, 1997 magnetic cloud. Geophysical Research Letters 25, 2995.

Lepping, R.P., Jones, J.A., Burlaga, L.F., 1990. Magnetic field structures of interplanetary magnetic clouds at 1 AU. Journal of Geophysical Research 95, 11 957.

Lepping, R.P., Acuna, M.H., Burlaga, L.F., Farrell, W., Slavin, J., Schatten, K., Mariani, F., Ness, N., Neubauer, F., Whang, Y.C., Byrnes, J., Kennon, R., Panetta, P., Scheifele, J., Worley, E., 1995. The WIND magnetic field investigation. Space Science Reviews 71, 207.

Lummerzheim, D., Brittnacher, M., Evans, D., Germany, G.A., Parks, G.K., Spann, J.F., 1997. High time resolution study of the hemispheric energy flux carried by energetic electrons in the ionosphere during the May 19/20, 1996 auroral activity. Geophysical Research Letters 24, 987.

Lysak, R.L., Lee, D.-H., 1992. The response of the dipole magnetosphere to pressure pulses. Geophysical Research Letters 19, 937.

Lysak, R.L., Song, Y., Grieger, J.C., 1995. Coupling of the magnetopause to the ionosphere by means of Alfvén waves and field-aligned currents. In: Song, P., Sonnerup, BUÖ., Thomsen, M.F. (Eds.), The Physics of the Magnetopause. American Geophysical Union, Washington, DC.

Lyons, L.R., Blanchard, G.T., Samson, J.C., Lepping, R.P., Yamamoto, T., Moretto, T., 1997. Coordinated observations demonstrating external substorm triggering. Journal of Geophysical Research 102, 27 039.

Mälkki, A., Eriksson, A.I., Dovner, P.-O., Böstrom, R., Holbeck, B., Holmgren, G., Koskinen, H.E.J., 1993. A statistical survey of auroral solitary waves and weak double-layers 1. Occurrence and net voltage. Journal of Geophysical Research 98, 15 521.

Ogilvie, K.W., Chornay, D.J., Fritzenreiter, R.J., Hunsaker, F., Keller, J., Lobell, J., Miller, G., Scudder, J.D., Sittler E.C. Jr., Torbert, R.B., Bodet, D., Needell, G., Lazarus, A.J., Steinberg, J.T., Tappan, J.H., Mavretic, A., Gergin, E., 1995. SWE, a comprehensive plasma instrument for the Wind spacecraft. Space Science Reviews 71, 55.

Olsen, J.V., Lee, L.C., 1983. PC1 wave generation by sudden impulses. Planetary and Space Science 31, 295.

Rostoker, G., Falthammar, C.-G., 1967. Relationship between changes in the interplanetary magnetic field and variations in magnetic field at the Earth's surface. Journal of Geophysical Research 72, 5853.

Rostoker, G., Jackel, B., Arnoldy, R.L., 1992. The relationship of periodic structures in auroral luminosity in the afternoon sector of ULF pulsations. Geophysical Research Letters 19, 613.

Russell, C.T., Wang, Y.-L., Raeder, J., Tokar, R.L., Smith, C.W., Ogilvie, K.W., Lazarus, A.J., Lepping, R.P., Szabo, A., Kawano, H., Mukai, T., Savin, S., Yermolaev, Yu., Zhou, X.-Y., Tsurutani, B., 2000. The interplanetary shock of September 24, 1998: arrival at Earth. Journal of Geophysical Research, in press.

Smith, E.J., Slavin, J.A., Zwickl, R.D., Bame, S.J., 1986. Shocks and storm sudden commencements. In: Kamide, Y., Slavin, J.A. (Eds.), Solar Wind–Magnetosphere Coupling. Terra Scientific Publishing Company, Tokyo, Japan.

Spann, J.G., Brittnacher, M., Elsen, R., Germany, G.A., Parks, G.K., 1998. Initial response and complex polar cap structures of the aurora in response to the January 10, 1997 magnetic cloud. Geophysical Research Letters 25, 2577.

Torr, M.R., Torr, D.G., Zukic, M., Johnson, R.B., Ajello, J., Banks, P., Clark, K., Cole, K., Keffer, C., Parks, G., Tsurutani, B., Spann, J., 1995. A far ultraviolet imager for the international solar-terrestrial physics mission. Space Science Reviews 71, 329.

Tsurutani, B.T., Arballo, J.K., Lakhina, G.S., Ho, C.M., Ajello, J., Pickett, J.S., Gurnett, D.A., Lepping, R.P., Peterson, W.K., Rostoker, G., Kamide, Y., Kokubun, S., 1998a. The January 10, 1997 auroral hot spot, horseshoe aurora and first substorm: a CME loop? Geophysical Research Letters 25, 3047.

Tsurutani, B.T., Arballo, J.K., Lakhina, G.S., Ho, C.M., Ajello, J.M., Pickett, J.S., Gurnett, D.A., Lepping, R.P., Peterson, W.-K., Rostoker, G., Kamide, Y., Kokubun, S., 1998b. A CME loop and the January 10, 1997 first substorm. In: Kokubun, S., Kamide, Y. (Ed.), Substorms-4. Kluwer Academic Publishers, Dordrecht.

Tsurutani, B.T., Gonzalez, W.D., 1997. The interplanetary causes of magnetic storms: a review. In: Tsurutani, B.T., Gonzalez, W.D., Kamide, Y., Arballo, J.K. (Eds.), Magnetic Storms. American Geophysical Union, Washington, DC.

Tsurutani, B.T., Kamide, Y., Arballo, J.K., Gonzalez, W.D., Lepping, R.P., 1999. Interplanetary causes of great and superintense magnetic storms. Physics and Chemistry of the Earth 24, 101.

Tsurutani, B.T., Lakhina, G.S., 1997. Some basic concepts of wave–particle interactions in collisionless plasmas. Reviews of Geophysics 35, 491.

Tsurutani, B.T., Lin, R.P., 1985. Acceleration of >47 keV ions and >2 keV electrons by interplanetary shocks at 1 AU. Journal of Geophysical Research 90, 12.

Zhou, X.-Y., Tsurutani, B.T., 1999. Rapid intensification and propagation of the dayside aurora: large scale interplanetary pressure pulses (fast shocks). Geophysical Research Letters 26, 1097.

Zhou, X.-Y., Tsurutani, B.T., 2000. Substorms, pseudobreakups and quiescent events caused by interplanetary shocks. Journal of Geophysical Research, submitted for publication.